DOI: 10.1002/anie.200803421

Quantum Dots

Biosensing and Probing of Intracellular Metabolic Pathways by NADH-Sensitive Quantum Dots**

*Ronit Freeman, Ron Gill, Itzhak Shweky, Moshe Kotler, Uri Banin, and Itamar Willner**

The use of semiconductor quantum dots (QDs) as optical labels for biorecognition events and biocatalytic processes attracts growing interest.[1,2] While numerous studies reported on the use of the QDs as fluorescent labels,[3–6] applications of semiconductor QDs as optical probes of dynamic bioprocesses, such as enzymatic transformations, using fluorescence resonance energy transfer (FRET) or photoinduced electron transfer reactions are still scarce. The replication of DNA by polymerase or telomerization of a nucleic acid by telomerase were monitored by the incorporation of a dye into the replica/telomers associated with QDs and the use of FRET as readout signal.[7] The scission of duplex DNA linked to CdSe QDs by DNase[8] and the hydrolytic cleavage of peptides bound to CdSe QDs[9,10] were followed by FRET processes. Recently, the activities of tyrosinase and thrombin were analyzed by the tyrosinase-induced generation of quinone residues on amino acid or peptide capping layers associated with CdSe QDs.[11] This resulted in electron-transfer quenching of the QDs. The subsequent hydrolytic cleavage of the peptide by thrombin removed the quencher and recovered the fluorescence of the QDs.

We describe the synthesis of Nile-blue-functionalized CdSe/ZnS quantum dots as a hybrid material that optically senses 1,4-dihydronicotinamide adenine dinucleotide (phosphate) cofactors, NAD(P)H. The modified quantum dots enable the fluorescence imaging of 1,4-nicotinamide adenine dinucleotide (phosphate) {$NAD(P)^+$}-dependent biocatalytic transformations and allow the monitoring of the intracellular metabolism in HeLa cancer cells. This technique allows the application of the NAD(P)H-sensitive QDs to screen anticancer agents and to probe the effect of drugs on intracellular metabolism.

Whereas previous applications of QDs to probe enzyme activities required the synthesis of specifically functionalized QDs, we sought generic functionalized QDs that could act as versatile probes to analyze different biocatalyzed transformations. Numerous redox enzymes use the common $NAD(P)^+$ cofactor, and hence the use of appropriately functionalized QDs to analyze NAD(P)H could provide a generic method to analyze $NAD(P)^+$-dependent enzymes, as well as to detect their substrates. Indeed, substantial efforts have been directed to the development of biosensors based on $NAD(P)^+$-dependent biocatalysts.[12]

Different enzyme electrodes for the amperometric detection of the substrates of $NAD(P)^+$-dependent enzymes were designed, and molecular electron relays[13] or redox polymers[14,15] were used to electrocatalyze the oxidation of NAD(P)H. Also, different integrated electrodes consisting of surface-confined relay–$NAD(P)^+$–enzyme assemblies for the electrochemical analysis of different substrates were developed.[16,17] Recently, the NAD(P)H-stimulated growth of Au nanoparticles was used to develop optical sensors that probe NAD^+-dependent enzymes and their substrates in solution or on surfaces.[18] Similarly, the NADH-mediated growth of Cu nanoparticles was used for the electrochemical detection of $NAD(P)^+$-dependent enzymes and their substrates.[19] Herein we report the design of functionalized semiconductor QDs for the detection of NADH and their use to follow NAD^+-dependent biocatalyzed transformations. Furthermore, we incorporated the NADH-sensing QDs into HeLa cancer cells and monitored the intracellular metabolism by the functionalized QDs and the effect of anticancer drugs on the cell metabolism.

CdSe-core CdS(2 layers, Ls)/$Cd_{0.5}$ $Zn_{0.5}$S(3 Ls)/ZnS(2 Ls) multishell QDs with diameter 7.3 ± 1.0 nm (core diameter 2.6 nm) were prepared according to a literature procedure.[11,20] These QDs were then transformed into water-soluble QDs by ligand exchange with 3-mercaptopropionic acid (MPA). The modified QDs were functionalized with bovine serum albumin (BSA), and then, Nile blue (**1**) was covalently linked to the BSA layer (see the Experimental Section). Spectroscopic analysis of the **1**-functionalized QDs indicated that approximately seven units of **1** were associated with each particle. Nile blue acts as an electron mediator for the oxidation of the NAD(P)H cofactors.[21] Accordingly, Figure 1a depicts the method to analyze NAD(P)H by the functionalized QDs. The fluorescence of the QDs is quenched by **1** through FRET quenching (QD emission: 635 nm, **1** absorbance: 630 nm). It should be noted that the quantum yield of emission of photoexcited **1** is very low at room temperature and cannot be detected. Thus, although **1** quenches effectively the luminescence of the QDs, it is non-emissive. In the presence of NADH, the reduced dye units (**2**) associated with the QDs lack absorbance in the visible spectral region, and thus do not quench the QDs. As a result, the reduction of the **1** capping layer by the NAD(P)H cofactors activates the fluorescence of the QDs, and provides a path for the optical detection of NADH. Figure 1b depicts the fluorescence intensity of the **1**-functionalized QDs prior

[*] R. Freeman, R. Gill, Dr. I. Shweky, Prof. M. Kotler, Prof. U. Banin, Prof. I. Willner
Institute of Chemistry and Center for Nanoscience and Nanotechnology
The Hebrew University of Jerusalem, Jerusalem 91904 (Israel)
Fax: (+972) 2-6527715
E-mail: willnea@vms.huji.ac.il
Homepage: http://chem.ch.huji.ac.il/willner

[**] This research is supported by the Converging Technologies Project, Israel Science Foundation. We thank Shira Winograd for her help with the synthesis of the quantum dots.

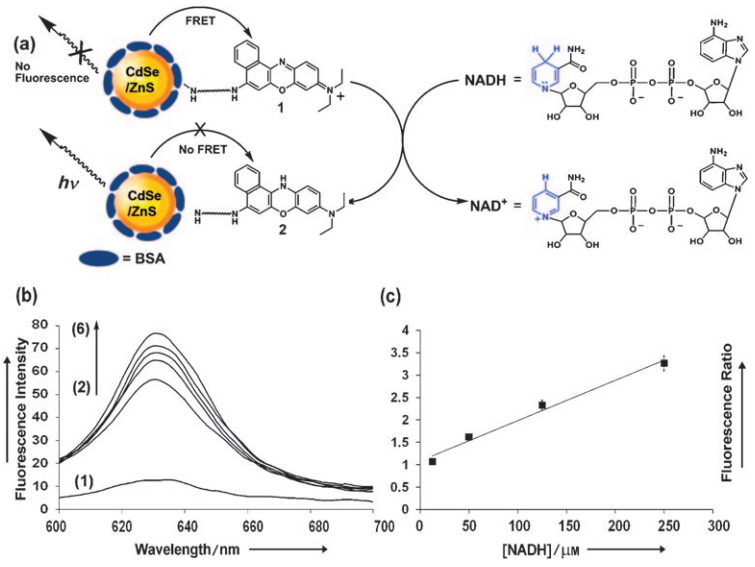

Figure 1. a) Sensing of NADH by Nile-blue-functionalized CdSe/ZnS QDs. b) Time-dependent fluorescence changes as a result of the interaction of the functionalized QDs with 0.5 mM NADH: (1) before addition of the NADH; (2) to (6) after successive time intervals of 3 min. c) Fluorescence intensity ratios of the modified QDs after the addition of different concentrations of NADH and the fluorescence intensities prior to the addition of NADH. (Fluorescence intensities after addition of NADH were recorded after a constant time interval of 15 min.) The samples included 50 nM QDs in a 10 mM phosphate buffer (pH 8.8).

The ability to analyze the NADH cofactor with QDs enabled the use of the QDs as luminescent probes to study the activity of NAD^+-dependent enzymes as well as their substrates. As a model system, the QDs were applied to analyze ethanol in the presence of the NAD^+-dependent alcohol dehydrogenase (AlcDH) (Figure 2a). In this system, AlcDH catalyzes the oxidation of ethanol to acetaldehyde with concomitant reduction of NAD^+ to NADH. The resulting reduced cofactor reduces the **1**-functionalized QDs, which leads to an increase in the fluorescence of the QDs. Figure 2b shows the time-dependent fluorescence changes of the QDs upon their treatment with 1 mM ethanol in the presence of NAD^+/AlcDH. As the reaction time intervals are prolonged, the quenching degree decreases (after 18 min the fluorescence intensity increases by 45%). Control experiments revealed that the fluorescence of the QDs was unaffected by excluding NAD^+ or AlcDH from the system, implying that all the components are essential to activate the fluorescence changes of the QDs. These results are consistent with the fact that AlcDH catalyzes the oxidation of ethanol with concomitant generation of NADH. The resulting reduced cofactor is oxidized by the quencher units **1** associated with the QDs, and as a result, the luminescence from the QDs is intensified. The ethanol-mediated formation of NADH in the presence of AlcDH enables the quantitative analysis of ethanol (Figure 2c). The biocatalyzed oxidation of different concentrations of ethanol was allowed to proceed in the presence of NAD^+/AlcDH for 18 min. As the concentration of ethanol increases, the concentration of

to the reaction with NADH [curve (1)] and the time-dependent fluorescence changes of the QDs upon reaction with 0.5 mM NADH [curves (2–6)]. As the time of the reaction is prolonged, the fluorescence is intensified, which is consistent with the increased reduction of the quencher units associated with the QDs. This situation is also reflected by the longer luminescence lifetime of the **1**-modified QDs after treatment with NADH (lifetime of the **1**-functionalized QDs is 3.5 ns prior to the reaction and 6.2 ns after treatment with 0.25 mM NADH for 15 min), implying that the resulting **2** modifying units do not quench the QDs. Figure 1c depicts the calibration curve that corresponds to the fluorescence intensities of the QDs upon treatment with different concentrations of NADH for 15 min. As the concentration of NADH increased, the fluorescence intensities of the QDs were enhanced. The primary modification of the QDs with albumin prior to the attachment of Nile blue is essential to construct the functional sensing QDs. We found that the direct coupling of Nile blue to the QDs yields inactive particles, because oxidized Nile blue (**1**), as well as reduced Nile blue (**2**), quench the luminescence of the QDs by reductive or oxidative electron-transfer mechanisms. The spatial separation of Nile blue from the QDs, using BSA, makes the electron-transfer quenching inefficient, whereas an energy-transfer quenching efficiency of around 90% allows the use of the QDs as luminescent probes.

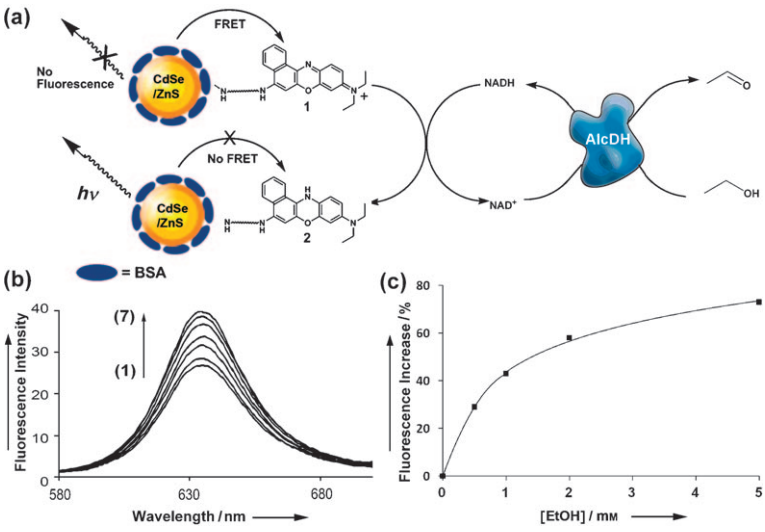

Figure 2. a) Sensing of ethanol by Nile-blue-functionalized CdSe/ZnS QDs. b) Time-dependent fluorescence changes for the analysis of 1 mM ethanol by the functionalized QDs: (1) prior to the addition of ethanol, (2) to (7) after successive time intervals of 3 min. c) Calibration curve corresponding to the optical analysis of different concentrations of ethanol by the functionalized QDs. Each sample was analyzed after reaction of the functionalized QDs for 18 min. The samples included 50 nM QDs in 10 mM phosphate buffer (pH 8.8).

the resulting NADH is higher, and consequently, the fluorescence of the QDs is intensified.

The successful analysis of the NAD(P)H cofactors suggested that the intracellular levels of NAD(P)H generated by the glycolysis and the Kreb's cycle could be monitored by the QDs, thus probing, in vitro, the active intracellular metabolism. Particularly, the enhanced metabolism in cancer cells[22] results in an increase of the NADH levels, and thus the functionalized QDs could probe the metabolic pathways in these cells and the effect of anticancer agents on the cellular metabolism. The **1**-functionalized QDs were incorporated into HeLa cancer cells by electroporation. Figure 3a shows a fluorescence image of a HeLa cell after the delivery of the QDs into the cell cytoplasm. The resulting cells retained viability and were kept in a growth medium that included 25 mM glucose (4.5 g L^{-1}) (see the Experimental Section for the detailed procedures). Curve (1) in Figure 3b depicts the fluorescence intensity of the HeLa cells after injection of 50 mM D-glucose into the growth medium. The insets show the fluorescence intensity images of a cell immediately after the addition of D-glucose, and after the intracellular metabolism was allowed to progress for 40 min. Clearly, the fluorescence intensity is enhanced, which is consistent with the fact that NADH was generated by the cell metabolism upon the addition of glucose. These fluorescence changes (±5%) were observed for different cell images (monitored for 20 different cells). Curve (2) in Figure 3b shows the time-dependent fluorescence of the QDs-labeled cells upon introduction of L-glucose to the growth medium. The fluorescence stays constant, which is consistent with the fact that L-glucose is not recognized by the cellular enzymes. These results imply that the changes in the fluorescence do not originate from a direct interaction of glucose with the QDs, but from the increase of NADH levels as a result of the D-glucose-induced intracellular metabolic pathway.

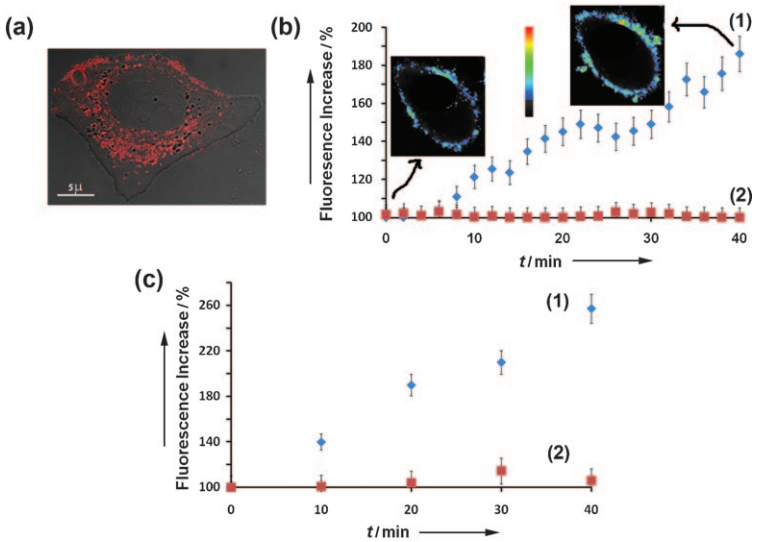

Figure 3. a) Confocal fluorescence microscope image of a HeLa cell that included incorporated Nile-blue-functionalized QDs. b) (1) Time-dependent fluorescence changes of HeLa cells that include the functionalized QDs upon interaction with 50 mM D-glucose. (2) Time-dependent fluorescence changes of HeLa cells that include the functionalized QDs upon interaction with 50 mM L-glucose. Each data point corresponds to the analysis of 20 different cells. Inset: the fluorescence image of one representative cell before and after the interaction with D-glucose. c) Time-dependent fluorescence changes of HeLa cells that include functionalized QDs upon addition of 50 mM D-glucose to (1) nontreated HeLa cells, and (2) taxol-treated HeLa cells. (Each of the data points represents the averaging of the results obtained from 20 individual cells.)

The fact that intracellular metabolism of cancer cells is regulated by anticancer agents, such as taxol, suggested that the NADH-sensitive CdSe/ZnS QDs may be used as optical sensors for anticancer drugs, and thus may provide a method for the screening of such drugs. Indeed, previous studies reported that the inhibition of the intracellular metabolism of A549 cancer cells by taxol could be monitored by fluorophore-labeled glucose derivatives acting as substrates.[23] Accordingly, HeLa cells that included the CdSe/ZnS-NADH-sensitive QDs were placed in six wells. Three of these wells were subjected to 9.8 μM taxol for 8 h, and all of the wells were then treated with 50 mM D-glucose. Curve (1) in Figure 3c shows the time-dependent fluorescence changes of individual HeLa cells that were not subjected to taxol in the three different wells. Curve (2) in Figure 3c shows the time-dependent fluorescence changes of the taxol-treated cells in three different wells. Evidently, taxol suppresses the metabolism in the cancer cells, thus leading to inefficient yields of NADH and lower fluorescence intensities of the QDs. These results imply that the functionalized QDs may be used for screening anticancer drugs that affect the intracellular metabolism. (It should be noted that taxol has no effect on the luminescence of the CdSe/ZnS QDs.)

To summarize, the present study has introduced a new method to analyze NAD^+-dependent biotransformations by Nile-blue-modified CdSe/ZnS QDs. Besides the very broad applicability of these QDs to probe a wide class of enzymes and their substrates, the functionalized QDs were introduced as optical labels that follow intracellular metabolic pathways at the single-cell level. The use of the functionalized QDs to monitor drug effectiveness and cellular metabolism offers exciting opportunities for drug screening. At present, one of the major problems in the use of these functionalized QDs for sensing is the difficulty to reproduce the properties of the modified QDs. We found that the lifetime of the modified graded-shell QDs differs by up to 15% between different batches. Also, the loading of the albumin-functionalized QDs with Nile blue (**1**) resulted in average loading differences of 10 to 15%.

Experimental Section

Materials: Ultrapure water from a NANOpure Diamond (Barnstead Int., Dubuque, IA) source was used throughout the experiments. Bis(sulfosuccinimidyl)suberate (BS^3) was purchased from Pierce Biotechnologies. Dulbecco's modified eagle medium (DMEM), trypsin, penicillin/streptomycin, L-glutamine, fetal bovine serum

were purchased from Biological Industries, Beit Haemek, Israel. All other reagents were purchased from Sigma–Aldrich Inc. Cells were scanned by using a FV-1000 confocal microscope (Olympus, Japan) equipped with an IX81 inverted microscope. A 60×/1.3 oil immersion objective was used. The FV-1000 confocal system was equipped with an incubator (LIS, Switzerland) controlling temperature and CO_2 concentration. Time-lapse scanning was preformed for up to 8 h.

Growth of graded CdS/ZnS shell on CdSe nanoparticles by layer-by-layer growth method: Chemicals: Technical grade (90%) trioctylphosphine oxide (TOPO), technical grade (90%) trioctylphosphine (TOP), cadmium acetate hydrate (99.99+%), selenium powder (−100 mesh, 95%), anhydrous toluene (99.8%), cadmium oxide (99.99%), sulfur (99–100% powder), zinc oxide (100.00% powder), octadecene (ODE, 90%), oleic acid (OA, 90%) mercaptopropionic acid (MPA, 99%), and octadecylamine (ODA, 98%) were used.

Injection solutions: Three cation precursor solutions and one anion precursor solution were prepared for the graded-shell growth: A zinc precursor solution (0.1M) was prepared by dissolving ZnO (0.2034 g) in oleic acid (6.18 g) and ODE (18 mL) at 310°C. A cadmium precursor solution (0.1M) was prepared by dissolving CdO (0.3204 g) in oleic acid (6.18 g) and ODE (18 mL) at 240°C. A Zn/Cd (1/1) precursor solution (0.1M) was prepared by dissolving ZnO (0.1017 g) and CdO (0.1602 g) in oleic acid (6.18 g) and ODE (18 mL) at 300°C. A sulfur precursor solution (0.1M) was prepared by dissolving sulfur (0.1285 g) in ODE (40 mL) at 180°C .The precursor solutions were made under an Ar flow. After clear solutions were obtained, the Cd, Zn, and Cd/Zn injection solutions were kept at about 80°C, while the sulfur injection solution was allowed to cool to room temperature. For each shell growth, a calculated amount of a given precursor solution was injected with a syringe using standard air-free procedures.

$CdS/Zn_{0.5}Cd_{0.5}S/ZnS$ multishell growth (prepared following a literature procedure):[11,20] ODA (3.7 g) and ODE (9.45 g) were loaded into a 100 mL three-neck flask. The flask was heated to 100°C for 1 h under vacuum (with a mechanical pump) to remove residual moisture and air from the system and cooled to room temperature. CdSe core nanocrystals (2.6 nm in diameter, 5.7×10^{-7} mol of particles) dissolved in chloroform (18.7 mL) were added, and the system was kept at 100°C under vacuum for 30 min to remove chloroform and other volatile materials. Subsequently, the system was put under an Ar flow, and the reaction mixture was further heated to 235°C for the shell growth. The CdSe cores were coated with (nominally) 2 Ls of CdS, 3 Ls of $Zn_{0.5}Cd_{0.5}S$, and 2 Ls of ZnS (14 injections in total; L = monolayer). The reaction was monitored by extracting aliquots 4 min after the beginning of each injection and measuring the absorption and fluorescence spectrum of the solution. The time interval between each injection was 10 min. At the end of the experiment the solution was kept for another 30 min at 260°C for annealing and then cooled to room temperature. For purification, chloroform was added to the flask, and the particles were precipitated by acetone. The liquid was separated from the nanocrystals by centrifugation (10 min at 6000 rpm). The nanocrystals were redissolved in chloroform to measure the quantum yield.

Water solubilization of the QDs: Stock solution of MPA: MPA (400 μL, 4.59×10^{-3} mol) was added to methanol (10 mL), and then KOH (500 mg) was added. The MPA stock (200 μL) solution was added to the QDs (1.5 mL) in chloroform with an optical density of 1.5, and the solution was shaken. The chloroform solution was seen to flocculate and became turbid. Water (1.5 mL, pH 11–12) was added to the flocculent solution, which was shaken again. The QDs were then extracted from the water phase.

Preparation of Nile-blue-capped QDs[24]: The MPA-capped QDs were mixed with a 1000-fold excess of bovine serum albumin (BSA) in 10 mM HEPES buffer (pH 7.4) containing 10 mM 1-ethyl-3-[3-dimethylaminopropyl] carbodiimide hydrochloride (EDC), and the mixture was shaken for 1 h. Then, the QDs were purified by precipitation and the particles were subsequently dissolved in 10 mM HEPES buffer (pH 7.4). To the particles solution was added BS^3 (bis[sulfosuccinimidyl]suberate) stock solution (50 μL, 1 mg mL^{-1} in 10 mM HEPES buffer, pH 8), and the mixture was shaken for 15 min. Then the QDs were purified by precipitation, and the particles were subsequently dissolved in 10 mM HEPES buffer (pH 7.4). The resulting QDs solution was mixed with a 50-fold excess of stock solution of **1** (1 mg mL^{-1} in 3:2 ethanol/water), and the mixture was shaken for 16 h. Excess of **1** was removed by two successive precipitation steps of the QDs using NaCl and methanol followed by centrifugation at 1500 rpm for 1 min. The resulting QDs were dissolved in 1 mL of 10 mM phosphate buffer (pH 8.8).

Cell culture: HeLa cells were cultivated (37°C, 5% CO_2) in DMEM solution that included 10% fetal bovine serum, penicillin/streptomycin, and L-glutamine for at least 18 h. Trypsin (1 mL) was added to the resulting suspension (5 mL), and the cells were centrifuged (5 min, 1500 rpm) and resuspended in a 10 mM phosphate buffer (pH 7.4) for electroporation measurements. The cell concentration was determined by standard hemocytometry.

Electroporation: A Bio-Rad electrocell manipulator was used to deliver **1**-functionalized QDs to the HeLa cells. Approximately 10^6 cells were suspended in 10 mM phosphate buffer (400 μL, pH 7.4) with 250 μg mL^{-1} QDs. The electroporation charge was applied (single 150 V, 5 ms pulse), and after 10 min the cells were plated onto glass-bottom microwell dishes or onto a poly-L-lysine coated microslide 8 well in DMEM for 18 h. All steps were performed at 4°C. Before imaging, the culture medium was replaced by a fresh medium to remove any detached cells and extracellular QDs.

Received: July 15, 2008
Revised: August 31, 2008
Published online: December 3, 2008

Keywords: biosensors · enzymes · nanobiotechnology · nanoparticles · quantum dots

[1] I. L. Medintz, H. T. Uyeda, E. R. Goldman, H. Mattoussi, *Nat. Mater.* **2005**, *4*, 435–446.
[2] R. C. Somers, M. G. Bawendi, D. G. Nocera, *Chem. Soc. Rev.* **2007**, *36*, 579–591.
[3] E. R. Goldman, E. D. Balighian, H. Mattoussi, M. K. Kuno, J. M. Mauro, P. T. Tran, G. P. Anderson, *J. Am. Chem. Soc.* **2002**, *124*, 6378–6382.
[4] E. R. Goldman, G. P. Anderson, P. T. Tran, H. Mattoussi, P. T. Charles, J. M. Mauro, *Anal. Chem.* **2002**, *74*, 841–847.
[5] D. Gerion, F. Chen, B. Kannan, A. Fu, W. J. Parak, D. J. Chen, A. Majumdar, A. P. Alivisatos, *Anal. Chem.* **2003**, *75*, 4766–4772.
[6] J. E. Schroeder, I. Shweky, H. Shmeeda, U. Banin, A. Gabizon, *J. Controlled Release* **2007**, *124*, 28–34.
[7] F. Patolsky, R. Gill, Y. Weizmann, T. Mokari, U. Banin, I. Willner, *J. Am. Chem. Soc.* **2003**, *125*, 13918–13919.
[8] R. Gill, I. Willner, I. Shweky, U. Banin, *J. Phys. Chem. B* **2005**, *109*, 23715–23719.
[9] I. L. Medintz, A. R. Clapp, F. M. Brunel, T. Tiefenbrunn, H. T. Uyeda, E. L. Chang, J. R. Deschamps, P. E. Dawson, H. Mattoussi, *Nat. Mater.* **2006**, *5*, 581–589.
[10] L. Shi, V. De Paoli, N. Rosenzweig, Z. Rosenzweig, *J. Am. Chem. Soc.* **2006**, *128*, 10378–10379.
[11] R. Gill, R. Freeman, J.-P. Xu, I. Willner, S. Winograd, I. Shweky, U. Banin, *J. Am. Chem. Soc.* **2006**, *128*, 15376–15377.
[12] I. Katakis, E. Dominguez, *Microchim. Acta* **1997**, *126*, 11–32.
[13] I. Willner, A. Riklin, *Anal. Chem.* **1994**, *66*, 1535–1539.
[14] O. A. Raitman, V. I. Chegel, A. B. Kharitonov, M. Zayats, E. Katz, I. Willner, *Anal. Chim. Acta* **2004**, *504*, 101–111.
[15] P. N. Bartlett, P. R. Birkin, E. N. K. Wallace, *J. Chem. Soc., Faraday Trans.* **1997**, *93*, 1951–1960.

[16] A. Bardea, E. Katz, A. F. Bückmann, I. Willner, *J. Am. Chem. Soc.* **1997**, *119*, 9114 – 9119.
[17] M. Zayats, E. Katz, I. Willner, *J. Am. Chem. Soc.* **2002**, *124*, 14724 – 14735.
[18] Y. Xiao, V. Pavlov, S. Levine, T. Niazov, G. Markovich, I. Willner, *Angew. Chem.* **2004**, *116*, 4619 – 4622; *Angew. Chem. Int. Ed.* **2004**, *43*, 4519 – 4522.
[19] B. Shlyahovsky, E. Katz, Y. Xiao, V. Pavlov, I. Willner, *Small* **2005**, *1*, 213 – 216.
[20] R. Xie, U. Kolb, T. Basche, A. Mews, *J. Am. Chem. Soc.* **2005**, *127*, 7480 – 7488.
[21] A. Malinauskas, T. Ruzgas, L. Gorton, L. T. Kubota, *Electroanalysis* **2000**, *12*, 194 – 198.
[22] R. A. Medina, G. I. Owen, *Biol. Res.* **2002**, *35*, 9 – 26.
[23] P. Jongmin, H. Y. Lee, M. H. Cho, S. B. Park, *Angew. Chem.* **2007**, *119*, 2064 – 2068; *Angew. Chem. Int. Ed.* **2007**, *46*, 2018 – 2022.
[24] A. M. Derfus, W. C. W. Chan, S. N. Bhatia, *Nano Lett.* **2004**, *4*, 11 – 18.

